Electronic and mechanical characterization of self-assembled alkanethiol monolayers by scanning tunneling microscopy combined with interaction-force-gradient sensing

U. Dürig,* O. Züger, and B. Michel
IBM Research Division, Zurich Research Laboratory, 8803 Rüschlikon, Switzerland

L. Häussling and H. Ringsdorf
Institut für Organische Chemie, Johannes-Gutenberg-Universität, 6500 Mainz, Germany
(Received 21 December 1992)

We have used scanning tunneling microscopy to study self-assembled monolayers of mercaptohexadecanol in ultrahigh vacuum. In addition to tunneling, the interaction force gradient acting between tip and sample was measured. Analysis of the force-gradient data shows that the tip is in mechanical contact with the surface of the monolayer which, in turn, is elastically compressed. The lateral dimensions of the mechanical contact are substantially (approximately five times) larger than the width of the tunneling-current filament. The results suggest that the compression of the monolayer constitutes an integral part of tunneling through the molecules. This view is further supported by spectroscopic measurements showing that the density of states at the Fermi level as seen by tunneling depends on the initial tunneling voltage used to define the gap width.

I. INTRODUCTION

Since the invention of the scanning tunneling microscope (STM) much interest has been directed towards investigating organic molecules.[1] One of the most striking observations was that tunneling experiments could be performed on organic materials known to be excellent macroscopic insulators such as Langmuir-Blodget films[2] and paraffin crystals.[3] Despite the vast amount of work being done in the field, little progress has been made in solving the fundamental problems related to electron conduction as seen by the STM.

Most of the experiments on organic materials have been carried out under ambient conditions. Contamination of the surface, in particular multilayer coverage with water, is likely to complicate the interpretation of results. This problem is avoided in ultrahigh vacuum (UHV) experiments. An ideal system for such investigations is provided by self-assembled monolayers (SAM's) of alkylmercaptanes HS-$(CH_2)_n$-OH on Au(111) substrates.[4] The molecules are arranged in a two-dimensional hexagonal lattice which is stabilized by van der Waals forces acting between the molecules and by a chemical bond of the sulfur head group to the Au substrate.[5]

As an explanation for the unexpected conductivity in organic molecules it has been speculated that the tip-sample pressure might play a key role.[6] It is therefore essential to measure both tunneling characteristics and mechanical properties of the tip-sample contact at the same time. To this end we have set up a UHV experiment using the method of force gradient sensing in combination with normal tunneling microscopy.[7] Results of our experiments performed on mercaptohexadecanol monolayers will be reported in this paper.

II. MATERIALS AND EXPERIMENTAL METHODS

Thin ($\simeq$2500 Å) (111)-oriented Au films epitaxially grown on cleaved mica served as substrates for the SAM's of mercaptohexadecanol[8] [HS-$(CH_2)_{16}$-OH, MHD]. Specimens were prepared by dipping the substrates in a $3.1\times10^{-4}M$ solution of MHD in absolute ethanol for 20 h. Upon removal from the solution the sample was thoroughly rinsed with pure solvent and blown dry with argon. Reproducibility of the preparation technique was checked by contact angle measurements performed on test samples as described in Ref. 8. Immediately after preparation, the specimens were transferred to the UHV-STM ($p<3\times10^{-10}$ mbar) through an air lock and investigated within 24 h.

In order to perform force-gradient measurements simultaneously while tunneling, the tip is mounted on a cantilever spring (CB). Its resonance frequency is shifted in proportion to the gradient of the interaction force acting between tip and sample. The resonance frequency of the CB is measured by means of the oscillator method described in detail in Ref. 7.

The CB-tip assembly was made of a wedge-shaped piece of W sheet metal with a thickness of 0.05 mm. The length and opening angle of the wedge were $\simeq$7 mm and $\simeq$8°, respectively. The pointed end of the wedge was electrochemically etched to form the tunneling tip. Finally the wedge was bent into an L-shape about 2 mm from the apex. Spring constant and resonance frequency of the assembly were determined experimentally. Typical values were $C=700$ Nm^{-1} and $f_0=1.5$ kHz, respectively. Final tip forming was performed *in situ*. In a first step the tip was resistively heated to $\simeq$1000 °C in order to remove surface contaminations. In a second step the

0163-1829/93/48(3)/1711(7)/$06.00

apex was shaped by the following procedure. A positive bias was applied to the tip using a constant current source. The current was set to 10 μA and the maximum tip voltage was limited to 100 V. The tip was first brought into contact with an Ir test sample. Then the gap width was slowly increased until the current dropped below the detection threshold ($\simeq$10 pA). Stable tips obtained by this method exhibited no anomalies of the *I-V* characteristics nor of the barrier height when tunneling on clean metal surfaces.

III. RESULTS AND DISCUSSION

A. Force-gradient characteristics

In a first set of experiments we measured the interaction force gradient and tunnel resistance as a function of tip-sample distance z at a fixed position on the sample. Since z cannot be determined unambiguously, we define it as the displacement of the tip with respect to a reference position which is given by a specific value of the tunnel resistance, typically between $R_T=10^9$ and 10^8 Ω. With the tip at the reference position, the feedback loop which adjusts for a constant tunneling current is interrupted and the tip is displaced first towards and then away from the surface over a predetermined z range. The resonance frequency and the tunneling current are simultaneously recorded during the entire ramp cycle. After each cycle the feedback loop is turned on for 100 ms to compensate for possible drifts.

As a reference example we show in Fig. 1 the result of such a measurement taken on a sputter-cleaned Ir sample. Initial tunneling conditions were $I_T=0.1$ *n*A and $V_T=25$ mV (tip bias measured with respect to sample). The curves represent averages over 32 ramp cycles. Only approach curves are shown as no differences could be detected between approaching and retracting from the surface. The interaction force gradient is *negative* and increases in absolute value with decreasing gap width as expected for the interaction of a metal tip with a metal surface.[9] This property provides a reliable test for the cleanliness of the tip as any kind of nonmetallic contamination will make the interaction force gradient positive. The tunnel resistance exhibits a nearly perfect exponential distance dependence with a barrier height of 5.3 eV, a value which is approximately equal to the mean vacuum work function of Ir and W.

The interaction force gradient measured on MHD samples is dramatically different from that of the previous example. The results of two consecutive experiments with different initial tunneling conditions $R_T=10^9$ and 10^8 Ω($V_T=100$ mV) are shown in Figs. 2(a) and 2(b), respectively. Large and *positive* values of the interaction force gradient are measured indicating that the tip is making mechanical contact with the sample. Nevertheless, force-gradient and tunnel resistance curves were reproducible and showed no hysteresis between forward and backward scans. The interaction force gradient increases rather gradually with decreasing gap width, a fact that cannot be reconciled with the exponential distance dependence expected for a hard-core repulsion interaction. This suggests that the alkane monolayer is actually

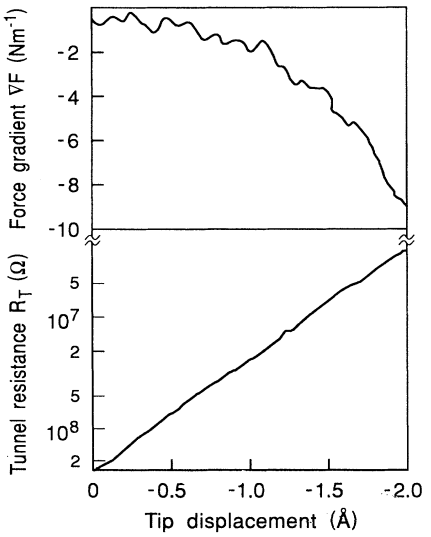

FIG 1. Force gradient ∇F and tunnel resistance R_T as a function of the gap width for a W tip and an Ir test sample. The gap width is defined as the displacement z of the tip with respect to a reference position corresponding to $R_T=3\times10^8$ Ω.

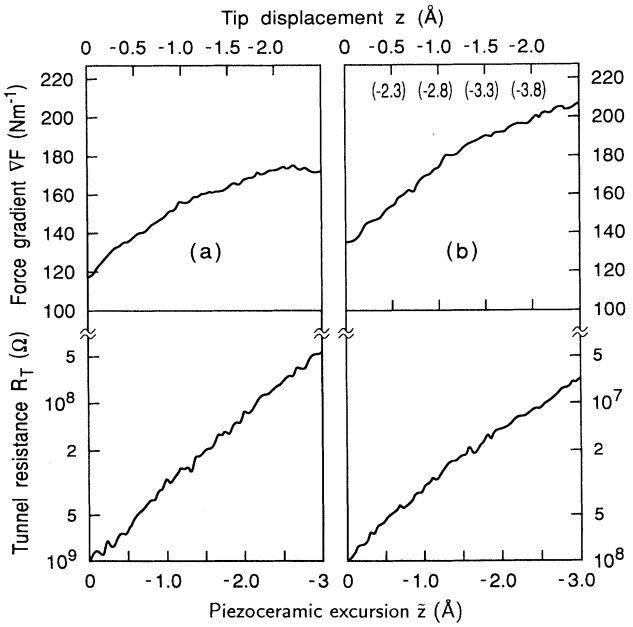

FIG. 2. Force gradient ∇F and tunnel resistance R_T as a function of gap width for a W tip and a self-assembled monolayer sample. The control parameter in the experiment is the displacement $\tilde{z}$ of the z piezoceramic to which the cantilever-spring-tip assembly is attached. The actual tip displacement z is obtained using Eq. (1) to compensate for the deflection of the spring. (a) Initial tunneling conditions: $I_T=0.1$ nA, $V_T=100$ mV. (b) Initial tunneling conditions: $I_T=1$ nA, $V_T=100$ mV. Numbers in parentheses on the tip-displacement scale correspond to renormalization to the initial conditions of (a).

elastically compressed by the tip. Thus the parameter z is basically a measure for the thickness of the alkane monolayer which acts as a spacing layer between tip and Au substrate.

The control parameter in the experiment is the excursion $\tilde{z}$ of the z piezoceramic, to which the CB-tip assembly is attached. Hence, in order to obtain the actual displacement of the tip with respect to the sample, we have to correct for the CB deflection by means of the following transformation:

$$z=\int_0^{\tilde{z}}\frac{C}{C+\nabla F(\tilde{z})}d\tilde{z}\ , \tag{1}$$

where ∇F and C denote the interaction force gradient and the spring constant of the CB, respectively. The correction is negligible as long as ∇F is small compared to C as is the case in the reference example (Fig. 1). With the SAM as the sample the difference between control parameter and tip displacement is appreciable as can be seen from Fig. 2.

We now inspect the tunnel current characteristics. Using the corrected tip excursion scale a nearly constant tunnel barrier height of 1.8 eV is obtained for $R_T \gtrsim 10^8\ \Omega$. For smaller values of R_T the barrier height decreases, gradually reaching a value of 0.8 eV at $R_T=10^7\ \Omega$. In terms of the tunneling current the measurements shown in Fig. 2 are complementary. Curves (a) and (b) match perfectly in the span where the respective tunnel resistances overlap. Hence we can renormalize the tip excursion scale in Fig. 2(b) (numbers in parentheses) with respect to the same initial conditions as in Fig. 2(a), viz. $R_T=10^9\ \Omega$, by adding -1.8 Å, which is the value of the tip excursion for $R_T=10^8\ \Omega$ in Fig. 2(a).

For the discussion of the force-gradient data we first recall the results of a recent Monte Carlo simulation directed at investigating the mechanical properties of SAM's of hexdecyl mercaptan, HS-$(CH_2)_{15}$-CH_3.[10] Those authors found that the monolayer can be elastically compressed over a range of $\simeq 3$ Å whereby the compliance is typically of the order of $\simeq 5\ \mathrm{Nm}^{-1}$ per molecule. We expect similar elastic properties for our SAM samples which are made of almost identical molecules with the exception of an alcohol end group. From the measured interaction force gradient which is of the order of 150 Nm^{-1} we thus infer that the tip-sample contact zone comprises approximately 30 molecules. This is equivalent to a contact diameter of $\simeq 30$ Å (based on a packing density of 21.6 Å^2 per molecule).

Neglecting shear forces, the tip-sample interaction force gradient due to elastic compression of the monolayer can be expressed as[9]

$$\nabla F(s)=2\pi R f(s)-2\pi\int_s^0 f(z')dz'\ . \tag{2}$$

Here R denotes the radius of curvature of the tip apex and s is the depth to which the tip indents the SAM. The term $f(s)$ denotes the restoring force per unit area for a uniform compression of the SAM normal to the surface. The depth s minus a constant offset determined by the initial tunneling parameters corresponds to the experimental tip excursion scale z. The second term in Eq. (2) can be neglected as long as $R \gg s$, a condition that is almost certainly fulfilled. Hence the force gradient ∇F probed by the tip is proportional to f.

The simple contact model does not adequately account for the experimental data, however. According to the simulations [see Fig. 4(b) in Ref. 10] the restoring force f increases first linearly and then parabolically with increasing compression whereas the experimental ∇F curves level off for large values of z. The discrepancy could arise because the pressure exerted by the tip on the SAM is confined to a small contact area comprising on the order of 30 molecules whereas it is assumed in the simulation that the pressure is applied uniformly on the entire surface. The relaxation of the molecular lattice is less constrained in the first case. It is conceivable that the stress is locally released by a combination of increasing the molecular tilt and the number of gauche defects in comparison with the respective value for uniform compression which all together would render the SAM less rigid on the nanometer scale.

By comparing the force gradient curves (a) and (b) in Fig. 2 one recognizes that, unlike the tunnel resistance curves, they cannot be matched. Considering the way the experiments were performed it becomes clear that the relaxation of the mechanical tip-sample contact involves processes with different time scales. Starting with a given tunnel resistance, say $10^9\ \Omega$ as in Fig. 2(a), the system was allowed to relax for several minutes before conducting the approach experiments. Raster scan images of the sample were recorded during the dwell time and we observed that the force gradient slowly settled at some value, 118 Nm^{-1} in this example, depending on R_T and other parameters—such as the detailed structure of the tip—that cannot be vigorously controlled in the experiment. Typically, the asymptotic value of the force gradient is larger, the smaller the value selected for the tunnel resistance. For values of R_T between 10^9 and $10^7\ \Omega$, interaction force gradients were measured ranging between 100 and 180 Nm^{-1}. The asymptotic interaction force gradient is, however, always smaller than the corresponding value measured in an approach experiment. Figure 2(a), for example, yields a force gradient of 170 Nm^{-1} for $R_T=10^8\ \Omega$. Letting the system subsequently relax with this value for R_T the force gradient eventually settled at 135 Nm^{-1} [see Fig. 2(b)]. From the absence of hysteresis in the rapid approach cycles we conclude that the slow relaxation process must evolve on a time scale $\gg 10$ s. One can further conclude that the overall contact force and the tunneling current are only partially correlated. This point will be elaborated in more detail later in the paper.

B. Force-gradient mapping

We also measured the interaction force gradient simultaneously while recording topographic images of the sample in the constant current operating mode of the STM. A typical example is shown in Fig. 3. Tunneling voltage and current are 100 mV and 1 nA, respectively. Several monoatomic terraces of the Au substrate can be recognized in Fig. 3(a). In addition, characteristic depressions

can be seen which are typical for self-assembled alkane monolayers.[4] Another characteristic are the telegraph-type height fluctuations producing the horizontal stripe pattern. All these topographic features also show up in the force-gradient map in Fig. 3(b), where dark and light tones correspond to 200 and 50 Nm^{-1}, respectively. Although there is no vigorous correlation, one can nevertheless say that the force gradient is generally larger at topographic depressions and smaller on protrusions irrespective of whether the topography is genuine or an artifact produced by noise.

Figure 4 is an enlargement of the area marked in Fig. 3, where (a) and (b) correspond to force gradient and topography, respectively. We first examine the Au step in more detail. Averages of the force gradient and the topography projected along the y axis of the box marked in Fig. 4 are depicted in Figs. 5(a) and 5(b), respectively. The force gradient gradually increases by approximately 30% as the step is approached. This increase is accompanied by a corresponding slight topographic depression. Conversely, the force gradient is reduced on top of the step and a small bump is observed in the topography. Nevertheless, a sharp transition from the lower to the upper terrace can be clearly discerned in the topographic signal—the resolution being approximately 10 Å.

In order to reconcile these features we must assume that the structure of the tip that supports the tunneling

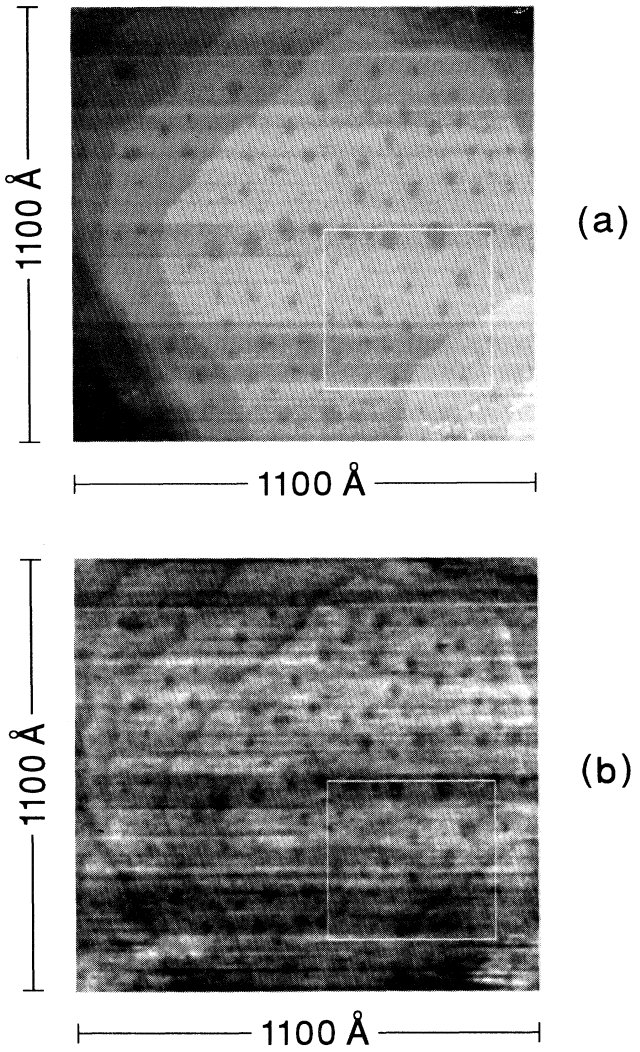

FIG. 3. (a) Topography and (b) force gradient (dark and light tones correspond to 200 and 50 Nm^{-1}, respectively) recorded on a self-assembled monolayer sample. Large monoatomic terraces of the Au substrate and characteristic pits can be recognized. The horizontal stripe pattern is caused by telegraph-type noise. Tunneling conditions are $I_T = 1$ nA, $V_T = 100$ mV.

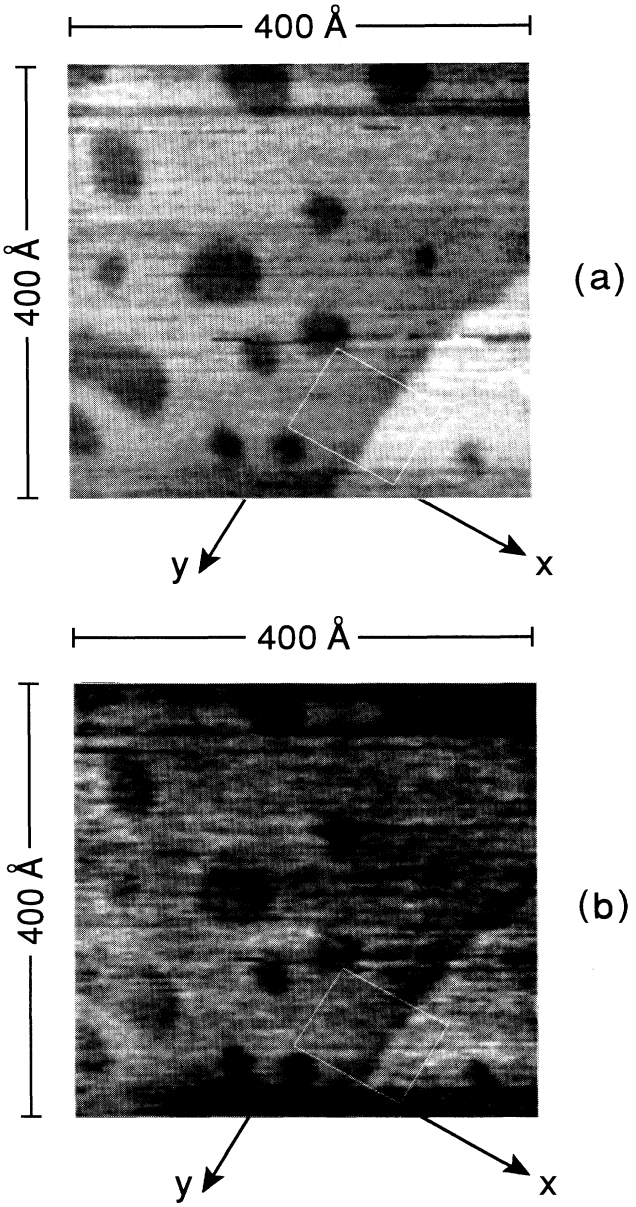

FIG. 4. (a) Topography and (b) force gradient recorded on the area marked by the box in Fig. 3.

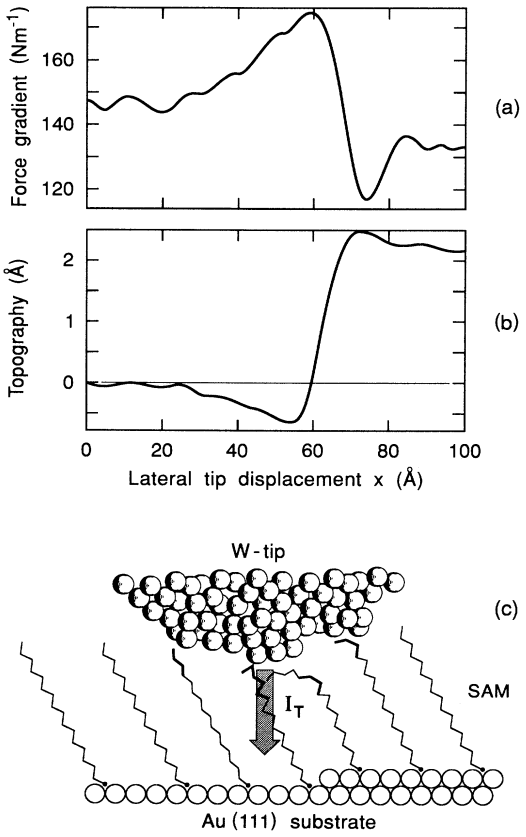

FIG. 5. Averages of the (a) topography and (b) force gradient projected along the y axis of the area marked by the box in Fig. 4. (c) Model of the tip-sample contact zone. Note that the tunneling current flows between an atomic asperity of the tip and the sample, thus the diameter of the current filament is about one order of magnitude smaller than the width of the mechanical contact zone. Thick lines indicate gauche defects.

current is substantially smaller than the actual mechanical contact area. The apex of the tunneling tip is almost certainly rough on an atomic scale. Hence it is conceivable that electrons tunnel out of that atomic protrusion on the tip apex which is closest to the Au surface [see Fig. 5(c)]. Hence we conclude that (1) the compression of the SAM by the tip varies substantially within the contact area and it is most likely highest where the tunneling current is flowing and (2) a precursor effect of the tip-sample interaction should be observed as the tip is traversing a sharp topographic step on the Au substrate.

Based on the above discussion the experimental data in Fig. 5 are interpreted as follows. Upon approaching the step on the lower terrace an additional repulsive force builds up as soon as the tip starts to compress the SAM on the upper terrace (at a lateral tip displacement $x \simeq 30$ Å). This process continues until the tunneling current filament itself reaches the step and the tip begins to retract according to the underlying topography ($x \simeq 60$ Å). At the same time the tip-sample interaction becomes weaker because the alkane molecules on the lower terrace are no longer in contact with the tip and the pressure on the alkane molecules on the upper terrace is released. Continuing the scanning motion of the tip the interaction force increases again until the entire contact area is embedded in the upper Au terrace ($x \simeq 80$ Å). According to this model one obtains a contact diameter of the order of 50 Å, which is broadly consistent with the value inferred from the force-gradient characteristics (Fig. 2). The topographic features close to the Au step arise because of the mechanical response of the spring holding the tip. With a spring constant of 700 Nm^{-1} one calculates a maximum additional repulsive force of $\simeq 40$ nN next to the step. Using 50 Å for the contact diameter the additional pressure exerted by the tip on the molecules on the upper terrace is of the order of 0.5 nN per molecule. This value is about a factor of 2 smaller than what is predicted by simulations for a compression of the SAM by 2 Å [the height of a monoatomic step on the Au(111) surface]. The enhancement of the interaction force gradient by $\simeq 40$ Nm^{-1} also appears to be on the small side. On the other hand, the same reasoning can be invoked here as was put forward to explain the leveling off of the force-gradient curve.

The nearly circular topographic pits shall be discussed next. In cross section they look like rectangular trenches whose depth fluctuates by ± 0.5 Å around a mean value of 2.5 Å. An extensive analysis of several SAM samples revealed that the pits cover $14 \pm 2\%$ of the total surface. Moreover we observed that they could be moved by the tip whereby small pits would aggregate to from larger entities. This is clearly visible by comparing Fig. 4 and the corresponding inset in Fig. 3. In fact, the mean radius[11] of the pits in Fig. 3 is 15 Å whereas the corresponding value in Fig. 4 is 25 Å as a result of tip-induced clustering caused by repetitive scanning of the same sample area. Note, however, that the fraction of the surface covered by pits is not changed by this process.

The small difference between the depth of the pits and the step height on the Au substrate could be taken as an indication that the pits might originate from missing atoms in the Au surface layer. These defects would most likely be formed during the deposition process of the SAM. Using the same arguments as in the discussion of the monoatomic steps, it is clear that such pits would also give rise to a corresponding increase of the interaction force gradient.

An alternative explanation is also conceivable. It has been shown in simulations in Ref. 10 and in infrared spectroscopy experiments (Nuzzo, Korenic, and Dubois[5]) that roughly 15% of all molecules of the alkane monolayer contain conformational gauche defects which in turn make these molecules shorter. In addition, it has been found in more recent simulations[12] that, along boundaries of domains with different molecular tilt angles, clusters of molecules containing a particularly large number of gauche defects give rise to pits covering approximately the same fraction of the surface as is observed in the experiment. The tip-induced mobility of the pits can be well understood in terms of this model. The pressure exerted by the tip onto the SAM constantly creates new gauche defects preferentially at the surface of the monolayer[10] which are propagated as the tip is scanning across

the surface. In fact, we observed a preferential motion of the pits along the scan axis. In order to explain the topographic contrast one needs a tunneling mechanism that forces the tip to follow the surface of the SAM (and not just the surface of the Au substrate).

There is no compelling experimental evidence in favor of either of the two models, as many important questions lack unambiguous answers.[13] Nevertheless, a number of facts can be inferred from our experiments. One can definitely rule out surface conduction through a thick adsorbed water layer because of the UHV environment. Reversibility of the force-gradient characteristics suggests that the SAM is only moderately compressed. This, in turn, precludes the possibility that the tip actually penetrates the monolayer to such a degree that the electrons tunnel between tip and Au substrate directly through a vacuum gap. Further, it was shown that the resolution obtained in tunneling images is of the order of 10 Å and hence the tunneling current filament is spatially well confined. We also showed that the tip makes mechanical contact with the SAM and that the diameter of this contact is approximately five times larger than the diameter of the tunneling current filament. Thus we conclude that the atomic structure of the tip plays a crucial role in tunneling. The relevant mechanisms involved cannot be decisively assessed from the experimental data. However, it is quite clear that the pressure exerted *locally* on individual molecules plays a key role, e.g., inducing conformational disorder of the carbon bonds as observed in the simulations of Ref. 10. Correspondingly, the tunneling current would sensitively depend on the detailed atomic structure of the tip. The latter is most likely constantly changing, given the strong interaction between tip and SAM. This would provide a natural explanation for the telegraph noise observed.

C. Tunnel-current spectroscopy

To shed additional light on the tunneling process, current versus voltage characteristics (I-V characteristics) were measured at constant gap width. The experiments were performed in a similar way as the measurements of the tunnel current and force-gradient characteristics (see Sec. III A) except that the tunneling voltage instead of the vertical tip position was ramped. The solid and dashed curves in Fig. 6 correspond to different settings of the initial tunneling parameters, namely $I_T=0.1$ nA, $V_T=100$ mV and $I_T=1$ nA, $V_T=-50$ mV, respectively. A common feature of both curves is the rapid decrease of the differential tunnel resistance with increasing voltage. I-V characteristics recorded on clean Ir test samples also show this property (see inset in Fig. 6) but to a much lesser degree. From this we conclude that the density of current carrying states on the SAM is substantially quenched close to the Fermi energy E_F. This is distinctively manifested by the solid line corresponding to an initial tunneling voltage $V_T=100$ mV that also proved to be well adapted for STM imaging. Here a pseudogap is observed in the range $-100\text{ mV}\lesssim V_T\lesssim 20$ mV where the differential tunnel resistance is larger than the resistance defined by the initial conditions (1 GΩ). It is also

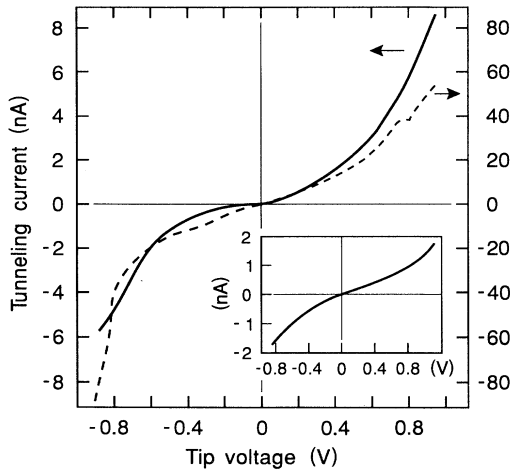

FIG. 6. Tunnel current vs tip bias voltage recorded on a self-assembled monolayer sample keeping the gap width constant. The gap width is defined by the initial tunneling conditions: $I_T=0.1$ nA, $V_T=100$ mV (solid line); $I_T=1$ nA, $V_T=-50$ mV (dashed line). For comparison an I-V characteristic measured on an Ir test sample is shown in the inset. Initial conditions are $I_T=0.1$ nA, $V_T=100$ mV.

evident from the curve that for small values of the bias voltage $-0.5\text{ V}\lesssim V_T\lesssim 0.5$ V tunneling out of filled sample states if favored.

We measured I-V spectra for different values of the initial tunneling voltage $-0.5\text{ V}\leq V_T\leq 0.5$ V. Characteristics similar to the solid curve were obtained for V_T values that were not within the pseudogap. In the opposite case, however, metallic-like I-V characteristics were observed close to E_F ($V_T=-50$ mV, dashed curve). At the same time a strong enhancement of the tunneling probability set in at a negative tip bias of $\simeq 0.8$ V indicating the presence of an empty sample state. We attempted to expand the voltage range in the I-V measurements in order to clarify this issue. It turned out, however, that the tunneling current abruptly started to fluctuate by at least one order of magnitude when the tip bias exceeded $\simeq\pm 1$ V (note that the gap width must be held constant in these measurements), rendering the collection of meaningful data impossible. In terms of the interaction force gradient no significant changes were noted between the two voltage regimes except for the general trend that the force gradient is larger, the smaller the selected tunnel resistance. This is to be expected in view of the locality of tunneling in comparison to the mechanical contact. Nevertheless, one might speculate that such a sample state could be induced by the local tip pressure and that the additional state density at E_F arises from a broadening of this state because of the coupling to the metallic tip.

IV. CONCLUSIONS

We have measured the tunnel resistance and the gradient of the force acting between a W tunneling tip and a sample consisting of a Au(111) substrate covered by a

monolayer of self-assembled mercaptohexadecanol molecules as a function of tip-sample distance. From the reversibility and the shape of the force-gradient characteristics we conclude that the tip elastically compresses the monolayer under normal tunneling conditions. Based on results from recent Monte Carlo simulations one infers that the mechanical contact area comprises on the order of 30 molecules. A careful analysis of force gradient and topography maps recorded at constant current allowed us to prove that the diameter of the tip-sample contact is indeed of the order of 50 Å, consistent with the interpretation of the force-gradient characteristics. However, the resolution obtained in tunneling images is $\simeq 10$ Å. Thus we conclude that only a small fraction of the tip area which is in contact with the monolayer actually contributes to tunneling. Most likely the tunneling current is mediated by atomic-size asperities on the tip. Furthermore, we argued that the pressure exerted *locally* on individual molecules plays a key role in the conduction mechanism. Additional support for this notion is provided by spectroscopy measurements showing that the density of states at the Fermi level as probed in a tunneling experiment is influenced by the tunneling parameters which in turn have an effect on the tip-sample pressure.

ACKNOWLEDGMENTS

It is a pleasure to acknowledge stimulating discussions with J. I. Siepmann, who made us aware of the interesting mechanical properties of alkane monolayer films, and with Ch. Joachim. We would also like to thank H. Wolf for carefully reading the manuscript and U. Maier for invaluable technical assistance.

---

*Author to whom correspondence should be sent. Electronic address: drg@zurlvm1(bitnet)

[1]One of the first reviews of the subject can be found in G. Travaglini, M. Amrein, B. Michel, and H. Gross, in *Scanning Tunneling Microscopy and Related Methods,* Vol. 184 of *NATO Advanced Study Institute, Series E: Applied Science,* edited by R. J. Behm, N. Garcia, and H. Rohrer (Kluwer Academic, Dordrecht, 1990), p. 335.

[2]H. Fuchs, W. Schrepp, and H. Rohrer, Surf. Sci. **181**, 391 (1987); C. A. Lang, J. K. H. Hörber, T. W. Hänsch, W. M. Heckl, and H. Möhwald, J. Vac. Sci. Technol. A **6**, 368 (1988).

[3]B. Michel, G. Travaglini, H. Rohrer, C. Joachim, and M. Amrein, Z. Phys. B **76**, 99 (1989).

[4]L. Häussling, B. Michel, H. Ringsdorf, and H. Rohrer, Angew. Chem. Int. Ed. Engl. **30**, 569 (1991); Y.-T. Kim and A. J. Bard, Langmuir **8**, 1096 (1992); C. A. Widrig, C. A. Alves, and M. D. Porter, J. Am. Chem. Soc. **113**, 2807 (1991); D. Anselmetti, Ch. Erdelen, L. Häussling, B. Michel, W. Mizutani, H. Ringsdorf, H. Wolf, and J. Yang (unpublished).

[5]R. G. Nuzzo, B. R. Zegarski, and L. H. Dubois, J. Am. Chem. Soc. **109**, 733 (1987); A. Ulman, J. E. Eilers, and N. Tillman, Langmuir **5**, 1147 (1989); C. D. Bain and G. M. Whitesides, Adv. Mater. **4**, 110 (1989); R. G. Nuzzo, E. M. Korenic, and H. Dubois, J. Chem. Phys. **93**, 767 (1990).

[6]S. M. Lindsay, O. F. Sankey, Y. Li, C. Herbst, and A. Rupprecht, J. Phys. Chem. **94**, 4655 (1990).

[7]U. Dürig, O. Züger, and A. Stalder, J. Appl. Phys. **72**, 1778 (1992).

[8]Mercaptohexadecanol was synthesized from 1.6-hexadecanediol (Alderich) by HBr treatment. The ω-bromo-hexadecanol was separated from the disubstituted compound by flash chromatography in dichlormethane and converted to mercaptohexadecanol via the Bunte-Salt as described in L. Häussling, H. Ringsdorf, F.-J. Schmitt, and W. Knoll, Langmuir **7**, 1837 (1991).

[9]U. Dürig, O. Züger, and D. Pohl, Phys. Rev. Lett. **65**, 349 (1990), U. Dürig and O. Züger, *Proceedings of the NATO-ARW on Manipulation of Atoms under High Fields, Lyon, France, 1992,* Vol. 235 of *NATO Advanced Studies Institute Series E: Applied Sciences* (Kluwer Academic, Dordrecht, 1993), p. 271.

[10]J. I. Siepmann and I. R. McDonald, Phys. Rev. Lett. **70**, 453 (1993).

[11]We define the mean radius as the first moment of the radial autocorrelation function.

[12]J. I. Siepmann and I. R. McDonald, Langmuir (to be published).

[13]D. Anselmetti, Ch. Gerber, B. Michel, H. Rohrer, H. Wolf, and H. J. Güntherodt (unpublished): Recent combined tunneling and force microscopy experiments conducted at ambient conditions provide evidence that the pits are not intrinsic topographic features. Instead they arise because of a local tip-induced compression of the SAM in response to a decrease of the local tunneling probability.

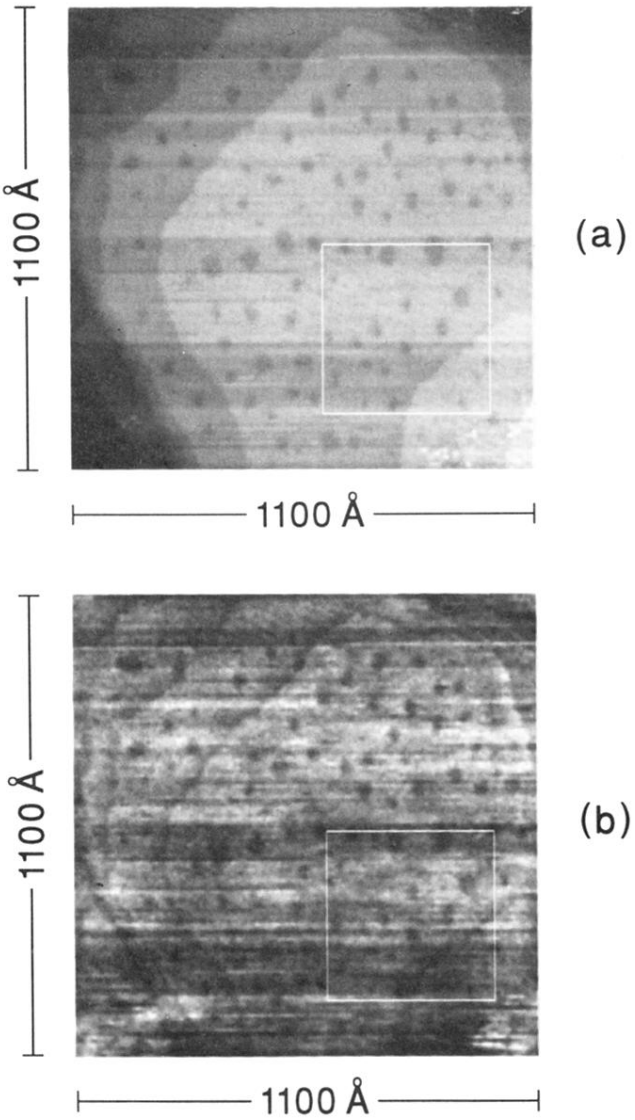

FIG. 3. (a) Topography and (b) force gradient (dark and light tones correspond to 200 and 50 Nm^{-1}, respectively) recorded on a self-assembled monolayer sample. Large monoatomic terraces of the Au substrate and characteristic pits can be recognized. The horizontal stripe pattern is caused by telegraph-type noise. Tunneling conditions are $I_T = 1$ nA, $V_T = 100$ mV.

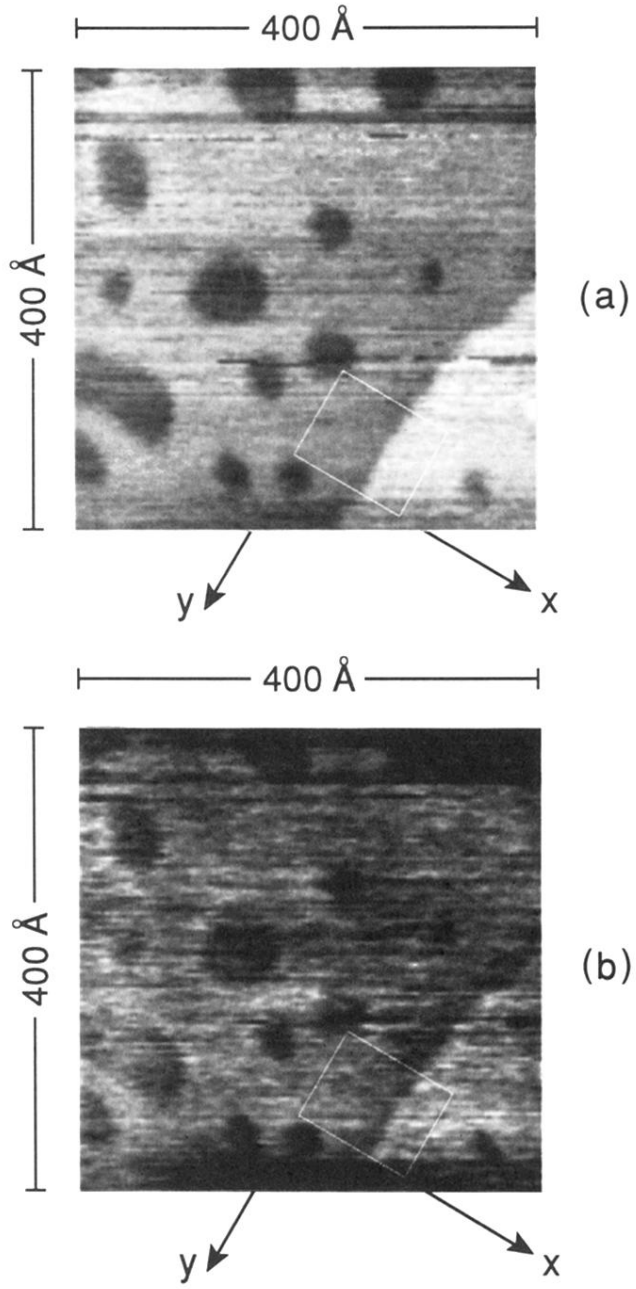

FIG. 4. (a) Topography and (b) force gradient recorded on the area marked by the box in Fig. 3.